Cell

Induction of Pluripotency in Mouse Somatic Cells with Lineage Specifiers

Jian Shu,[1,3,9] Chen Wu,[3,6,9] Yetao Wu,[3,6,9] Zhiyuan Li,[2,7,9] Sida Shao,[1] Wenhui Zhao,[1,3] Xing Tang,[4] Huan Yang,[3,6] Lijun Shen,[1] Xiaohan Zuo,[3,6] Weifeng Yang,[1] Yan Shi,[6] Xiaochun Chi,[5] Hongquan Zhang,[5] Ge Gao,[4] Youmin Shu,[8] Kehu Yuan,[8] Weiwu He,[8] Chao Tang,[2,3,*] Yang Zhao,[1,3] and Hongkui Deng[1,3,6,*]
[1]The MOE Key Laboratory of Cell Proliferation and Differentiation, College of Life Sciences
[2]Center for Quantitative Biology
[3]Peking-Tsinghua Center for Life Sciences
[4]College of Life Sciences, State Key Laboratory of Protein and Plant Gene Research, Center for Bioinformatics
Peking University, Beijing 100871, China
[5]Laboratory of Stem Cells, Development and Reproductive Medicine, School of Basic Medical Sciences, Peking University, Beijing 100191, China
[6]Laboratory of Chemical Genomics, School of Chemical Biology and Biotechnology, Peking University Shenzhen Graduate School, Shenzhen 518055, China
[7]Biophysics Graduate Program, University of California, San Francisco, San Francisco, CA 94158, USA
[8]OriGene Technologies, 9620 Medical Center Drive, Rockville, MD 20850, USA
[9]These authors contributed equally to this work
*Correspondence: tangc@pku.edu.cn (C.T.), hongkui_deng@pku.edu.cn (H.D.)
http://dx.doi.org/10.1016/j.cell.2013.05.001

SUMMARY

The reprogramming factors that induce pluripotency have been identified primarily from embryonic stem cell (ESC)-enriched, pluripotency-associated factors. Here, we report that, during mouse somatic cell reprogramming, pluripotency can be induced with lineage specifiers that are pluripotency rivals to suppress ESC identity, most of which are not enriched in ESCs. We found that *OCT4* and *SOX2*, the core regulators of pluripotency, can be replaced by lineage specifiers that are involved in mesendodermal (ME) specification and in ectodermal (ECT) specification, respectively. *OCT4* and its substitutes attenuated the elevated expression of a group of ECT genes, whereas *SOX2* and its substitutes curtailed a group of ME genes during reprogramming. Surprisingly, the two counteracting lineage specifiers can synergistically induce pluripotency in the absence of both *OCT4* and *SOX2*. Our study suggests a "seesaw model" in which a balance that is established using pluripotency factors and/or counteracting lineage specifiers can facilitate reprogramming.

INTRODUCTION

Understanding the establishment of cellular identity in programming and reprogramming is a major goal of modern biology. For years, pluripotency-associated factors and their rivals, lineage specifiers, have generally been considered to determine the identities of pluripotent and differentiated cells, respectively (Jaenisch and Young, 2008; Young, 2011). Accordingly, the reprogramming factors that induce pluripotency have been identified primarily from embryonic stem cell (ESC)-enriched factors, pluripotency-associated factors, or maternal factors such as *Oct4*, *Sox2*, *Klf4*, *c-Myc*, *Nanog*, *PRDM14*, *Sall4*, *Esrrb*, *Utf1*, *Tet2*, and *Glis1* (Aoi et al., 2008; Buganim et al., 2012; Chia et al., 2010; Doege et al., 2012; Maekawa et al., 2011; Maherali et al., 2008; Takahashi and Yamanaka, 2006; Yu et al., 2007). Likewise, the direct reprogramming of differentiated cells into other differentiated cell types has been successfully demonstrated by several lineage specifiers, such as *Gata4* and *Hnf4a* (Vierbuchen and Wernig, 2011). Thus, the perspective that the direct conversion of cell state A to cell state B should be realized by a set of master regulatory factors of cell type B has been a prevailing strategy (Graf and Enver, 2009; Jopling et al., 2011); however, whether this is the only strategy for cell fate conversion is unclear.

Recent data indicate that the most critical reprogramming factor, *Oct4*, which inhibits the expression of differentiation-related genes in ESCs (Kim et al., 2008; Pardo et al., 2010), is sufficient to direct the reprogramming of somatic cells into induced pluripotent stem cells (iPSCs) (Li et al., 2011; Zhu et al., 2010). Therefore, it is of great significance to find substitutes for *Oct4* to elucidate its physiological role and gain a better understanding of the reprogramming mechanisms, which remain largely unknown. The ESC-enriched factor *Nr5a2* has been identified as an *Oct4* substitute (Heng et al., 2010). However, the physiological role of *Oct4* remains unclear because *Nr5a2* directly regulates *Oct4* and binds to the upstream promoter region of *Oct4* (Gu et al., 2005; Guo and Smith, 2010). Therefore, extensively screening for novel *Oct4* substitutes among factors including but not limited to ESC-related factors may cast light on the molecular mechanisms that underlie reprogramming and pluripotency, thereby facilitating the development of safer and more efficient reprogramming strategies.

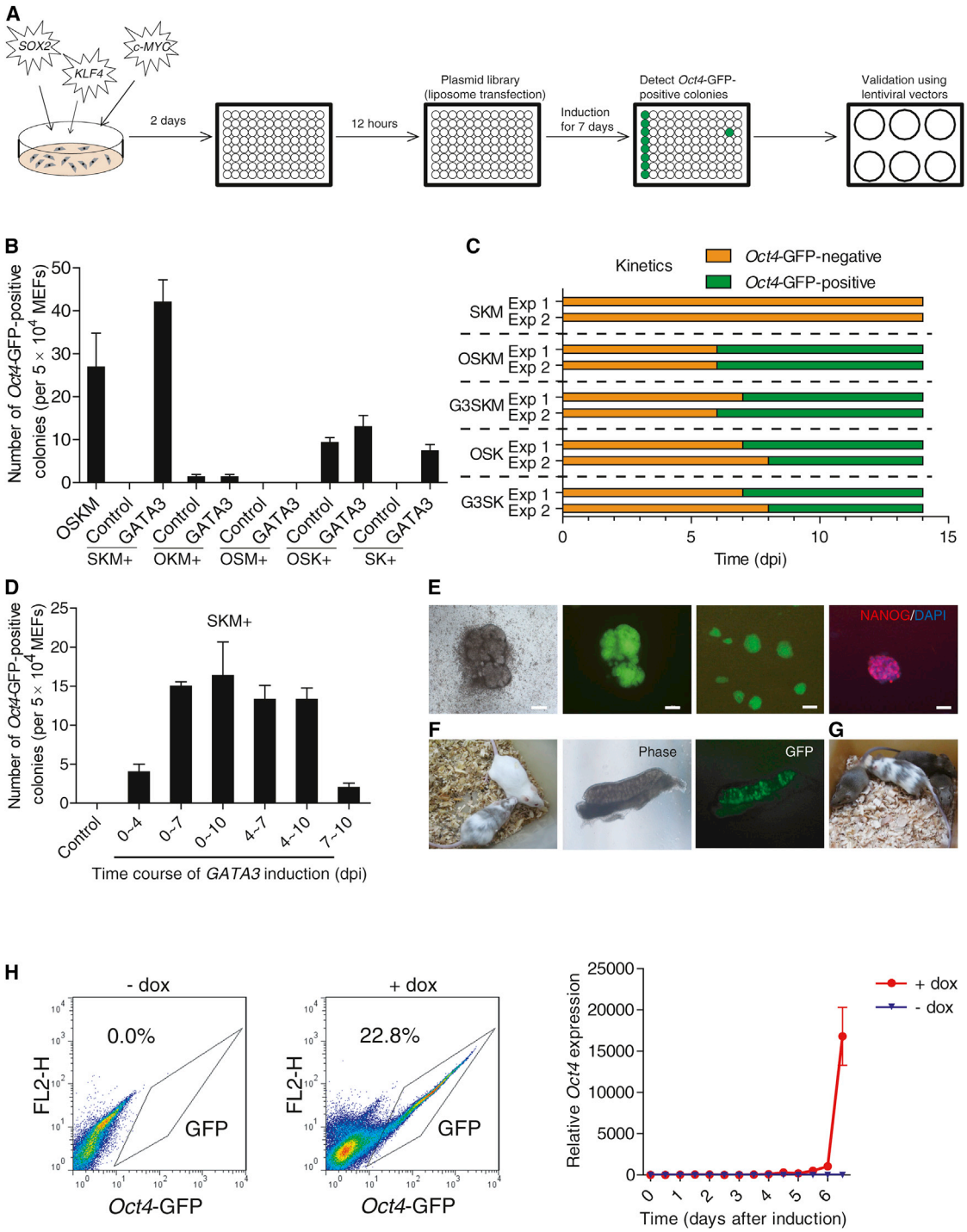

Figure 1. *GATA3* Can Substitute for *OCT4* to Induce Pluripotency in Mouse Somatic Cells

(A) Schematic representation of the gene-screening process. For the screen, a plasmid library of 10,080 human genes was analyzed. An *OCT4* plasmid and empty vectors (EV) were used as positive and negative controls in the first and second column, respectively.

(B) Reprogramming assay that determines the ability of the lineage specifier *GATA3* to enhance reprogramming in the absence of *OCT4*, *SOX2*, *KLF4*, or *c-MYC*. The *Oct4*-GFP-positive colonies were counted at 9 days postinfection (dpi). SKM, OKM, OSM, OSK, and SK plus EV were used as negative controls. OSKM was used as a positive control. Error bars indicate the SD (n = 3).

(C) The kinetics of reprogramming using different combinations of genes. For the 50,000 MEFs seeded per well, the GFP fluorescence was monitored every 24 hr. The orange bars indicate that no *Oct4*-GFP-positive cells were observed, whereas the green bars indicate the emergence of *Oct4*-GFP-positive cells. Two representative independent experimental sets are shown.

(legend continued on next page)

Here, we identified eight lineage specifiers as *OCT4* substitutes, including *GATA3*, *GATA6*, and *SOX7*, which are involved in mesendodermal (ME) lineage specification. *OCT4* and its substitutes attenuated the elevated expression of a group of ectodermal (ECT) genes, such as the ECT lineage specifier *Dlx3*, that were collectively triggered by *SOX2*, *KLF4*, and *c-MYC* (SKM). Knockdown of *Dlx3* enhanced reprogramming in the absence of *OCT4*, rather than in the absence of *SOX2*. In addition, *SOX2* can be replaced by lineage specifiers involved in ECT lineage specification, such as *GMNN*. Surprisingly, the two counteracting lineage specifiers can synergistically induce pluripotency in the absence of both *OCT4* and *SOX2*. We suggest a ''seesaw model'' in which the balance that is established by pluripotency factors and/or lineage specifiers facilitates the induction of pluripotency in somatic cells. This model could shed light on fundamental questions regarding the establishment of cellular identity during programming and reprogramming.

RESULTS

Induction of Pluripotency in Mouse Somatic Cells with *GATA3*

In our study, we screened an initial plasmid library of 10,080 human genes for their ability to replace *OCT4* when introduced together with virally expressed SKM to direct the reprogramming of mouse embryonic fibroblasts (MEFs) containing a green fluorescent protein (GFP) reporter driven by an *Oct4* promoter and enhancer. Reprogramming efficiency was evaluated by determining the number of *Oct4*-driven GFP-positive colonies. We found that *GATA3* had the most significant effect in the primary hits (Figure 1A and Table S1 available online). Interestingly, *GATA3* is not enriched in ESCs and is an important regulator of development and differentiation (Figure S1D and Table S4) (Ting et al., 1996).

We further validated the ability of *GATA3* to replace *OCT4* during the reprogramming of MEFs, mouse adult dermal fibroblasts (MDFs), mouse gastric epithelial cells (GECs), and mouse keratinocytes using viral vectors (Figures 1B, S1A, and S1B). The expression of exogenous genes was verified (Figure S1E). We found that *GATA3* achieved a reprogramming efficiency that was comparable to or even higher than that of *OCT4*. We subsequently evaluated the ability of *GATA3* to enhance reprogramming in the absence of *SOX2*, *KLF4*, or *c-MYC*. We observed that *GATA3* was also able to enhance reprogramming in the absence of *c-MYC*, but it was unable to substitute for *SOX2* or *KLF4* (Figure 1B). Next, we monitored the kinetics of *GATA3*- and *OCT4*-induced reprogramming. We found that *Oct4*-GFP-positive cells emerged at 6–7 days postinfection (dpi) during both *GATA3*- and *OCT4*-induced reprogramming (Figure 1C). We found that *GATA3* may mainly function at 4–7 dpi (Figure 1D), which corresponds to the period during which the pluripotency circuitry is reconstructed (Polo et al., 2012).

iPSCs Generated with *GATA3* Are Pluripotent

The iPSCs generated using *GATA3*, *SOX2*, *KLF4*, and *c-MYC* (G3SKM) had morphology similar to mouse ESCs (Figures 1E and S2A). The G3SKM-induced iPSCs were stable during long-term passaging and stained positive for alkaline phosphatase (AP), SSEA-1, UTF1, and NANOG (Figures 1E, S2A, and S2B). The methylation levels of the *Nanog* and *Oct4* promoters were similar to the methylation levels in mouse ESCs (Figure S2C). Genomic integrations of the viruses into the genomic DNA were confirmed in iPSCs, teratomas, and tissues from chimeric mice, and showed no *OCT4* transgene integration (Figure S2D). The expression of endogenous pluripotency-associated genes was activated, and the expression of exogenous *GATA3*, *SOX2*, *KLF4*, and *c-MYC* was silenced in these cells (Figure S2E), which indicates that they were fully reprogrammed. G3SKM-induced iPSCs produced germline-competent chimeras (Figures 1F and 1G), and these iPSCs were further validated by the characterization of teratoma formation, gene expression profiles, and other assays (Figures S2F and S2G and Tables S2).

GATA3 Has Little Effect on the Events Noted in Previous Studies

To identify the potential mechanisms by which *GATA3* could replace *OCT4*, we examined several pathways that have been reported to facilitate or inhibit reprogramming. To test whether *GATA3* could activate endogenous *Oct4* to a high level shortly after induction so that it was the activated endogenous *Oct4* plus SKM that induced pluripotency, we monitored the endogenous *Oct4* expression levels using doxycycline (dox)-inducible G3SKM-secondary MEFs (Wernig et al., 2008), 20%–40% of which could be reprogrammed. We did not detect significant *Oct4* activation until *Oct4*-GFP-positive cells had begun to emerge (Figure 1H). There was also no significant activation of the pluripotency-associated factor *Nanog* until *Oct4*-GFP-positive cells began to emerge (Figure S1C).

We found that *GATA3* had little effect on mesenchymal-epithelial transition (MET) (Figure 2A) (Li et al., 2010;

(D) The *Oct4*-GFP-positive colonies generated by dox-inducible *GATA3* and constantly expressed SKM were counted at 10 dpi. Dox was added to the culture medium for various periods of time to induce the expression of *GATA3*. SKM plus EV was used as a negative control. Error bars indicate the SD (n = 3).
(E) The generation of iPS colonies with G3SKM from *Oct4*-GFP MEFs. Phase and GFP images of a primary iPS colony, GFP images of passaged iPS colonies, and the expression of NANOG in iPS colonies are depicted from left to right. Scale bars, 100 μm.
(F) An adult chimeric mouse (left) generated from G3SKM-induced iPSCs (#1). Phase (middle) and GFP (right) images of the male gonads dissected from an E13.5 G3SKM-iPS-#1 chimeric embryo.
(G) Germline transmission mice (agouti) from #1 are depicted.
(H) The flow cytometric analysis of GFP in G3SKM-secondary MEFs without (left) and with (middle) dox. RT-qPCR analysis of the relative expression of endogenous *Oct4* in G3SKM-secondary MEFs in the process of dox induction. Representative results from three independent experiments are shown. Error bars indicate the SD (n = 3).
See also Figures S1 and S2 and Tables S1 and S2.

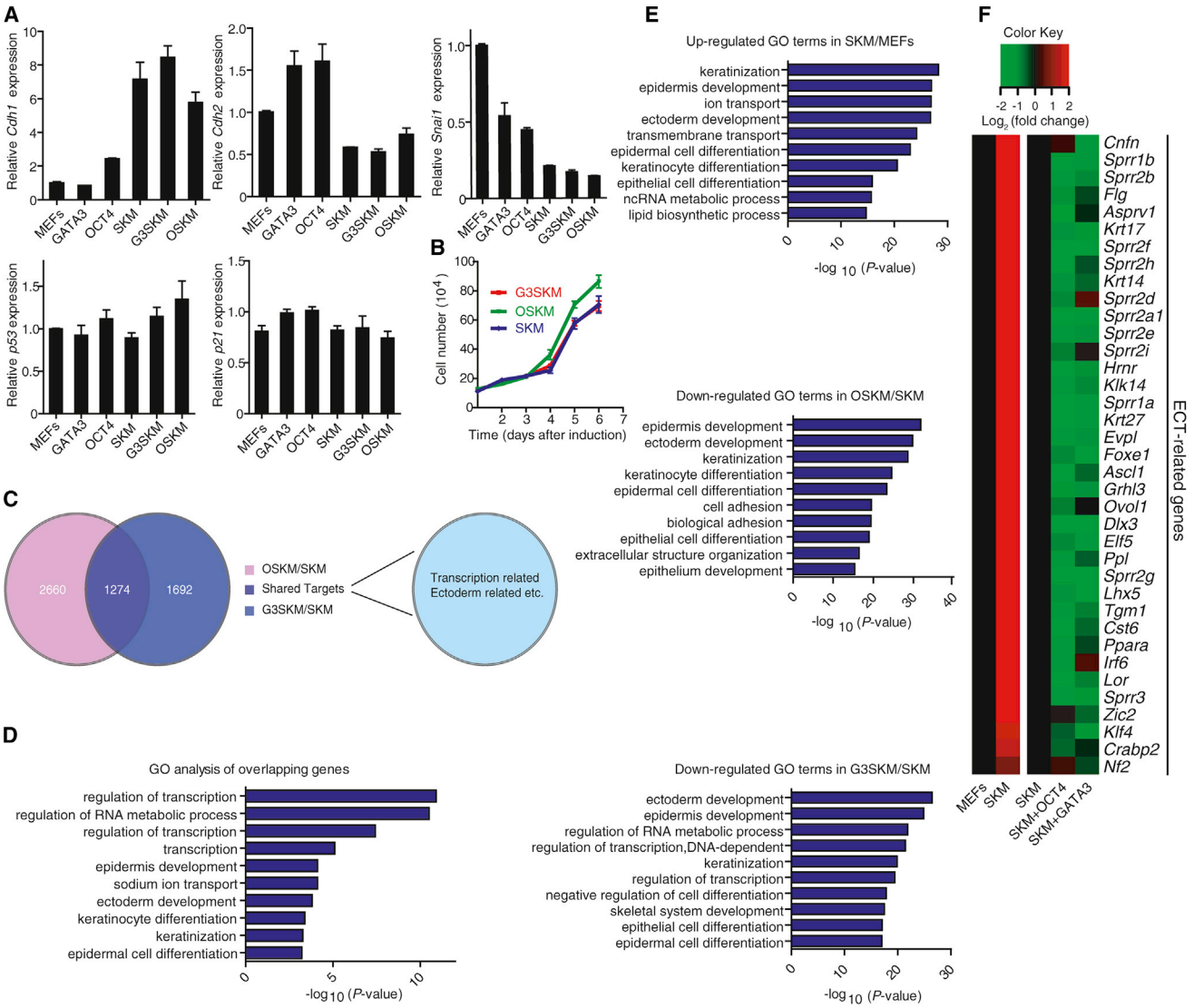

Figure 2. *OCT4* and *GATA3* Can Inhibit a Group of ECT Genes that Are Elevated by SKM during Reprogramming

(A) RT-qPCR analysis of the expression of endogenous *Cdh1*, *Cdh2*, *Snai1*, *p53*, and *p21* relative to their expression in MEFs. The samples were tested at 4 dpi. Error bars indicate the SD (n = 3).

(B) Cell proliferation curves. SKM was used as a control, and 50,000 MEFs were seeded per well. Three wells were harvested every 24 hr to count the number of cells. The cell populations were analyzed using a paired two-tailed Student's t test. No significant difference was observed between G3SKM- and SKM-infected MEFs ($p = 0.7803$). Error bars indicate the SD (n = 3).

(C) A Venn diagram illustrating the overlap between the expression changes identified in cells induced with G3SKM and OSKM. The blue circle represents the DE lists (expression change > 2-fold, $p < 0.05$, FDR < 0.01) in G3SKM-induced cells compared with SKM-induced cells. The purple circle represents the DE lists of OSKM-induced cells compared with SKM-induced cells.

(D) Gene ontology (GO) analysis of the overlapping genes in (C). The GO analysis was based on the DE list. The p values represent the Bonferroni-corrected EASE score.

(E) GO analysis of genes regulated by SKM, G3SKM, and OSKM at 7 dpi. The GO analysis was based on the DE list. The p values represent the Bonferroni-corrected EASE score.

(F) Heatmaps depicting the relative fold change of gene expression at 7 dpi based on the ECT-related genes by RNA-seq. Red and green indicate increased and decreased expression, respectively.

Samavarchi-Tehrani et al., 2010). In addition, *p53* and *p21* expression was not affected by *GATA3* (Figure 2A) (Zhao et al., 2008). Moreover, we did not observe any significant changes in cell proliferation (Figure 2B), which suggests that *GATA3* does not contribute to reprogramming by accelerating cell proliferation. These results suggest that *GATA3* functions in a manner different from the mechanisms noted in previous studies to promote reprogramming.

OCT4 and *GATA3* Inhibit the ECT-Related Genes that Are Elevated by SKM

To further determine the roles of *OCT4* and *GATA3* in inducing pluripotency, we performed RNA-sequencing (RNA-seq) assays at 7 dpi based on our kinetics test (Figures 1C and 1D). The shared targets of *OCT4* and *GATA3* were involved in several important processes, such as cell adhesion and the regulation of transcription, based on gene ontology (GO) function enrichment analysis (Figures 2C and 2D). Interestingly, we observed that, compared with MEFs, the upregulated genes that were most significantly enriched were related to ectoderm and epidermis development following the introduction of SKM. When *OCT4* and *GATA3* were introduced along with SKM, the most significantly enriched downregulated genes were also related to ectoderm and epidermis development (Figures 2E and 2F). These results suggest that SKM may have the potential to direct cells toward an ECT state and that the inhibition of ECT-related genes by *OCT4* and *GATA3* may facilitate the induction of pluripotency.

Screening of Other Lineage Specifiers as Substitutes for *OCT4*

The current model proposes that ESCs are maintained by a shield of pluripotency factors that collaboratively prohibit differentiation into any lineage to preserve an undifferentiated state (Boyer et al., 2005; Silva et al., 2009). A more recent and provocative perspective is that pluripotency factors function as classical lineage-specifying factors to direct the differentiation of ESCs into a specific lineage while inhibiting their commitment to mutually exclusive lineages (Loh and Lim, 2011). In ESCs, *Oct4* promotes ME and primitive endoderm differentiation and suppresses ECT differentiation (Niwa et al., 2000; Thomson et al., 2011; Wang et al., 2012). Interestingly, the overexpression of *Gata3* in ESCs directs primitive endodermal differentiation, and similar to *Oct4*, *Gata3* also functions in some ME lineages (Nishiyama et al., 2009). The similarity of *OCT4* and *GATA3* in lineage specification suggests that other lineage specifiers may also replace *OCT4*. To test this possibility, we screened several additional lineage specifiers using viral overexpression (Table S3). The results indicated that the lineage specifiers *GATA6*, *SOX7*, *PAX1*, *GATA4*, *CEBPa*, *HNF4a*, and *GRB2* were able to substitute for *OCT4* to induce pluripotency (Figures 3A, 3B, and S1E). These lineage specifiers have been shown to function mainly during multiple stages of ME differentiation and in early embryonic patterning (Table S4). Most of these substitutes for *OCT4* are not enriched in ESCs (Figure S1D). However, the lineage specifiers that are primarily involved in ectodermal lineage specification (e.g., *SOX1* and *ASCL1*) were unable to replace *OCT4* (Table S3).

Other *OCT4* Substitutes Also Inhibit ECT-Related Genes Elevated by SKM

Because both *OCT4* and *GATA3* attenuated the elevated expression of the group of ECT genes that was collectively triggered by SKM, we asked whether the other substitutes for *OCT4* could also attenuate their expression. We performed microarray assays to analyze the roles of other *OCT4* substitutes. In addition, we analyzed another lineage specifier, *MIXL1*, as a negative control, which could not replace *OCT4* despite its involvement in ME lineage specification. Consistent with our expectations, the other *OCT4* substitutes, but not *MIXL1*, attenuated the upregulation of ECT genes by SKM (Figure 3C). GO analysis also showed that the most significantly enriched downregulated genes after the introduction of *OCT4* substitutes other than *MIXL1* were associated with ectoderm and epidermis development and other terms related to ECT specification (Figure S3).

Next, to validate the tendency apparent from the RNA-seq and microarray analyses (Figures 2F and 3C), we performed real-time quantitative PCR (RT-qPCR) assays. We observed that typical ECT marker genes, such as *Dlx3* and *Lhx5*, were upregulated by SKM and significantly downregulated after the introduction of *OCT4* and its substitutes (Figures 3D). To further validate these findings, we performed single-colony assays. We acquired AP-positive, *Oct4*-GFP-negative colonies in different conditions, including controlled SKM conditions. Then, we mechanically split each colony into two subcolonies. We analyzed one subcolony for gene expression while tracing the other half subcolony in culture to monitor whether it became *Oct4*-GFP positive and dox independent (Figure S4). In this case, we could analyze those reprogramming-competent colonies that were headed toward pluripotency. AP-positive colonies grown in SKM conditions failed to become *Oct4*-GFP positive, suggesting that they are reprogramming refractory. We found a concomitant downregulation of *Dlx3* and *Lhx5* after the introduction of *OCT4* and its substitutes (Figure 3E). This finding is consistent with the results from mixed cell populations, supporting the lineage specification tendency observed in the bulk population. These results suggest that *OCT4* and its substitutes can repress the upregulation of ECT-related genes that are triggered by SKM.

Suppression of *Dlx3*, a Master ECT-Related Gene, Facilitates Reprogramming in the Presence of SKM

To test whether the inhibition of ECT-related genes by *OCT4* and its substitutes correlated with the promotion of reprogramming, we further evaluated whether the knockdown of the master ECT lineage-related genes that are upregulated by SKM could also promote reprogramming in the absence of *OCT4*. We found that the knockdown of the key ECT marker *Dlx3*, which subsequently resulted in the downregulation of several other ECT genes, promoted reprogramming in the absence of *OCT4*, rather than in the absence of *SOX2* (Figures 4 and S5), functionally supporting the data observed by gene profiling (Figures 2E, 2F, and 3C–3E). Furthermore, iPSCs generated with *Dlx3* shRNAs were proven to be pluripotent by stringent characterization assays (Figures 4E, 4F, and Table S2). We found no significant binding of *Oct4* and *Gata3* to the *Dlx3* promoter region in published ChIP data from "hmChIP," which suggests that *Oct4* and *Gata3* may indirectly regulate *Dlx3* (Figure S5D). Together, our data indicate that *OCT4* and its substitutes attenuate the upregulation of ECT-related genes that is triggered by the SKM combination; this inhibition correlates with facilitating the induction of pluripotency.

SOX2 and Its Substitutes Attenuate the Expression of ME-Related Genes Elevated by OKM

Similar to *Oct4*, *Sox2* also regulates lineage specification in ESCs. *Sox2* inhibits mesendodermal differentiation and

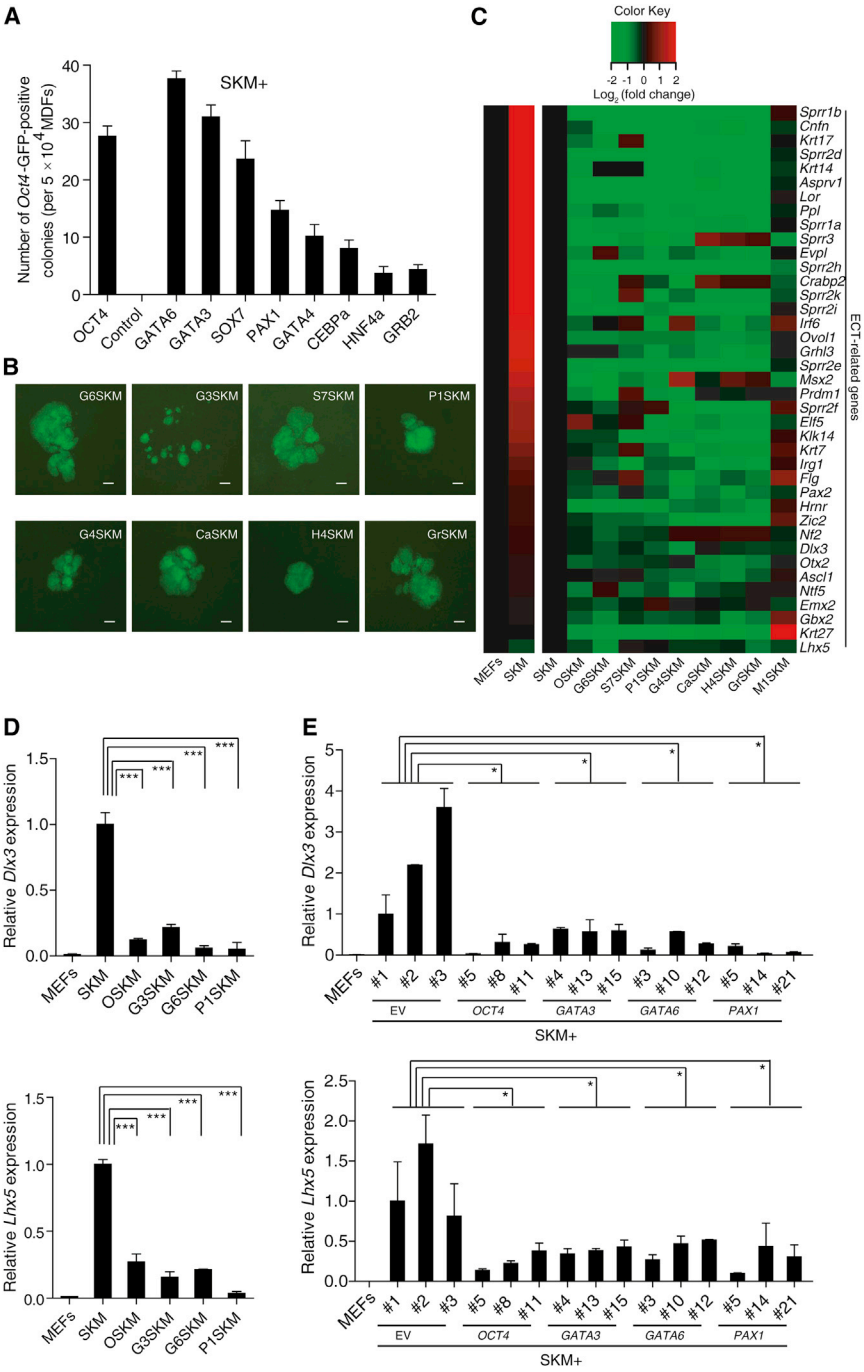

Figure 3. Identification of Other Substitutes for *OCT4* that also Inhibit ECT-Related Genes Elevated by SKM during Reprogramming

(A) Identification of additional lineage specifiers that are related to the ME lineage that can replace *OCT4* during reprogramming. The *Oct4*-GFP-positive colonies were counted at 9 dpi. SKM plus EV was used as a control. Error bars indicate the SD (n = 3).

(B) GFP images of iPS colonies generated with SKM+*GATA6* (G6SKM), SKM+*GATA3* (G3SKM), SKM+*SOX7* (S7SKM), SKM+*PAX1* (P1SKM), SKM+*GATA4* (G4SKM), SKM+*CEBPa* (CaSKM), SKM+*HNF4a* (H4SKM), and SKM+*GRB2* (GrSKM). Scale bars, 100 μm.

(C) Heatmaps depicting the relative fold change of gene expression at 7 dpi based on the ECT-related genes by microarray. Red and green indicate increased and decreased expression, respectively.

(D) RT-qPCR analysis of the expression of endogenous *Dlx3* (top) and *Lhx5* (bottom) relative to the expression in SKM. The samples were tested at 7 dpi after removal of *Oct4*-GFP-positive cells. Significance was assessed compared with the controls using a one-tailed Student's t test. ***p < 0.001. Error bars indicate the SD (n = 3).

(E) RT-qPCR analysis of the expression of endogenous *Dlx3* (top) and *Lhx5* (bottom) relative to the expression in SKM from a single colony; three colonies from each condition were tested. Significance was assessed compared with the controls using a one-tailed Student's t test. *p < 0.05. Error bars indicate the SD (n = 3).

See also Figures S3 and S4 and Tables S2, S3, S4.

promotes neural ectodermal differentiation (Thomson et al., 2011; Wang et al., 2012). Intuitively, we asked whether the lineage specifiers involved in ECT lineage specification could substitute for *SOX2* during reprogramming. Indeed, the previously identified *SOX2* substitutes, *Sox1*, *Sox3*, and *RCOR2*, are regulators of ECT development or are particularly expressed in neural tissues (Nakagawa et al., 2008; Tontsch et al., 2001; Yang et al., 2011; Zeng et al., 2010). In addition, we demonstrated that *GMNN*, which is involved in ECT lineage specification (Seo et al., 2005), could substitute for *SOX2* to promote reprogramming (Figures 5A, 5B, S1E, and Table S4).

To assess whether *SOX2* and its substitutes could attenuate the upregulation of the ME-related genes that are induced by *OCT4*, *KLF4*, and *c-MYC* (OKM), we performed microarray and RT-qPCR analyses. The expression of a group of classical ME markers was elevated after the induction of OKM; these elevated expression levels were attenuated by *SOX2* and its substitutes (Figures 5C and 5D). Furthermore, we performed similar single-colony assays as previously mentioned to test this tendency in reprogramming-competent cells. We observed that *SOX2* and its substitutes inhibited the expression of *T* and *Eomes* in these colonies (Figure 5E). These data indicate that *SOX2* and its substitutes attenuate the upregulation of ME-related genes that is induced by OKM during the reprogramming process.

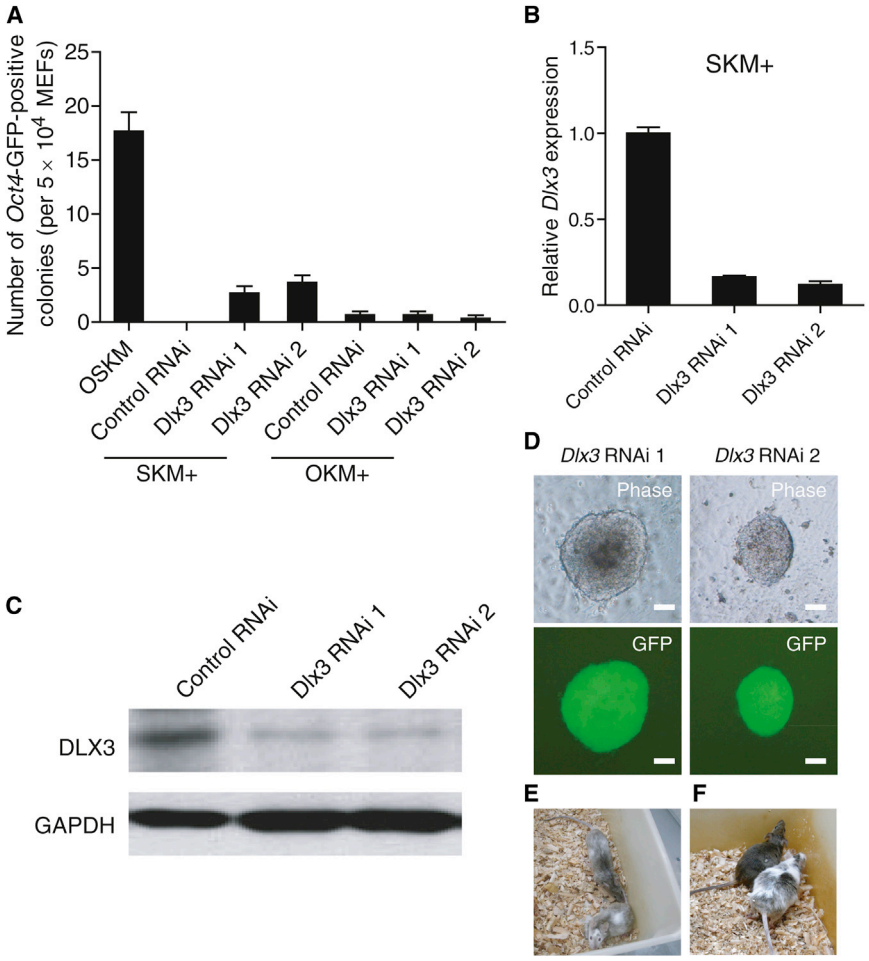

Figure 4. Inhibition of the Master ECT Gene *Dlx3* Facilitates Reprogramming in the Presence of SKM

(A) shRNAs targeting *Dlx3* were introduced into MEFs with SKM or OKM. Scrambled shRNA (control RNAi) was used as a control. The *Oct4*-GFP-positive colonies were counted at 9 dpi. Error bars indicate the SD (n = 3).

(B) RT-qPCR analysis of the expression of endogenous *Dlx3* relative to the expression in control. SKM plus scramble shRNA (control RNAi) was used as a control. The samples were tested at 7 dpi. Error bars indicate the SD (n = 3).

(C) Western blot analysis of DLX3 in control and knockdown cells in the presence of a SKM virus cocktail. GAPDH was used as a loading control.

(D) Phase and GFP images of iPS colonies generated with *Dlx3* RNAi 1 and *Dlx3* RNAi 2 in the presence of SKM. Scale bars, 100 μm.

(E) Adult chimeric mice generated from *Dlx3* RNAi 2-induced iPSCs (#1).

(F) A germline transmission mouse (agouti) from #1 is depicted.

See also Figure S5.

A "Seesaw Model" Suggests that the Balancing of Counteracting Forces Facilitates the Induction of Pluripotency

A two-node model of cell fate determination has been studied in various instances of pluripotent stem or progenitor cells that undergo a binary cell fate decision (e.g., *GATA1* and *PU.1*, *RUNX2*, and *PPARg*) (Huang, 2009). This circuit has already hinted at the concept of a "balanced pluripotent state" (Figures S6A and S6B). To better understand the induction of pluripotency by lineage specifiers, we propose a "seesaw model" (Figures 6A and 7) based on previous studies (Hanna et al., 2009; Loh and Lim, 2011; Niakan et al., 2010; Niwa et al., 2000; Polo et al., 2012; Rosa and Brivanlou, 2011; Teo et al., 2011; Thomson et al., 2011; Wang et al., 2012) and our current data (Figures 2, 3, 4, 5, S3, S4, and S5). This model consists of two coupled modules: the pluripotency module and the differentiation module. The pluripotency module is represented by the mutual activation of *Oct4* and *Sox2*, whereas the differentiation module is modeled by mutually inhibiting the ME and ECT genes (Figure 6A).

Simulations of the model produced three cell states: the pluripotency state, the ME state, and the ECT state (Figures 6B and S6C). In somatic states, the pluripotency state is unreachable (Figure 6C, box i). However, overexpression of *KLF4* and *c-MYC* (KM) may act as a driving force that reduces reprogramming barriers (Polo et al., 2012), so the pluripotency state becomes a local attractor that is reachable from a somatic state if properly perturbed (Figure 6C, box ii). Note that the pluripotent state is most easily reached (high pluripotency potential) if the expression strengths of the ME and ECT genes are forced to be in the blue region, i.e., if they are balanced.

A key result of this model is that pluripotency and reprogramming can be achieved by a variety of perturbations to the system, as illustrated in Figure 6D. For example, the overexpression of *SOX2* alone will switch on the ECT genes that inhibit the pluripotency module, in turn bestowing the ECT state onto the cell, regardless of the initial cell state (Figures 6D, box i, S6I, and S6N). The overexpression of *OCT4* (or the ME gene *GATA3*) in combination with *SOX2* counteracts the inhibition of the ECT genes to the pluripotency module, which permits the cell to move into the pluripotency attractor region (Figures 6D, boxes ii and iii, S6D, and S6E). More strategies for restoring pluripotency as suggested by the model are shown in Figures 6D and S6 and Tables S5 and S6.

Some of the results from our model are consistent with previous studies (Table S6). Deviation from the balanced equilibrium for pluripotency directs cells to flow into divergent differentiated states. For example, the enforced expression of *OCT4* results in cellular transdifferentiation into mesodermal hematopoietic cells (Szabo et al., 2010). *SOX2*, SKM with neural lineage specifiers, and reduced *Oct4* expression in the OSKM cocktail can result in neuroectodermal lineage transdifferentiation from fibroblasts (Han et al., 2012; Ring et al., 2012; Thier et al., 2012). Other strategies identified by our

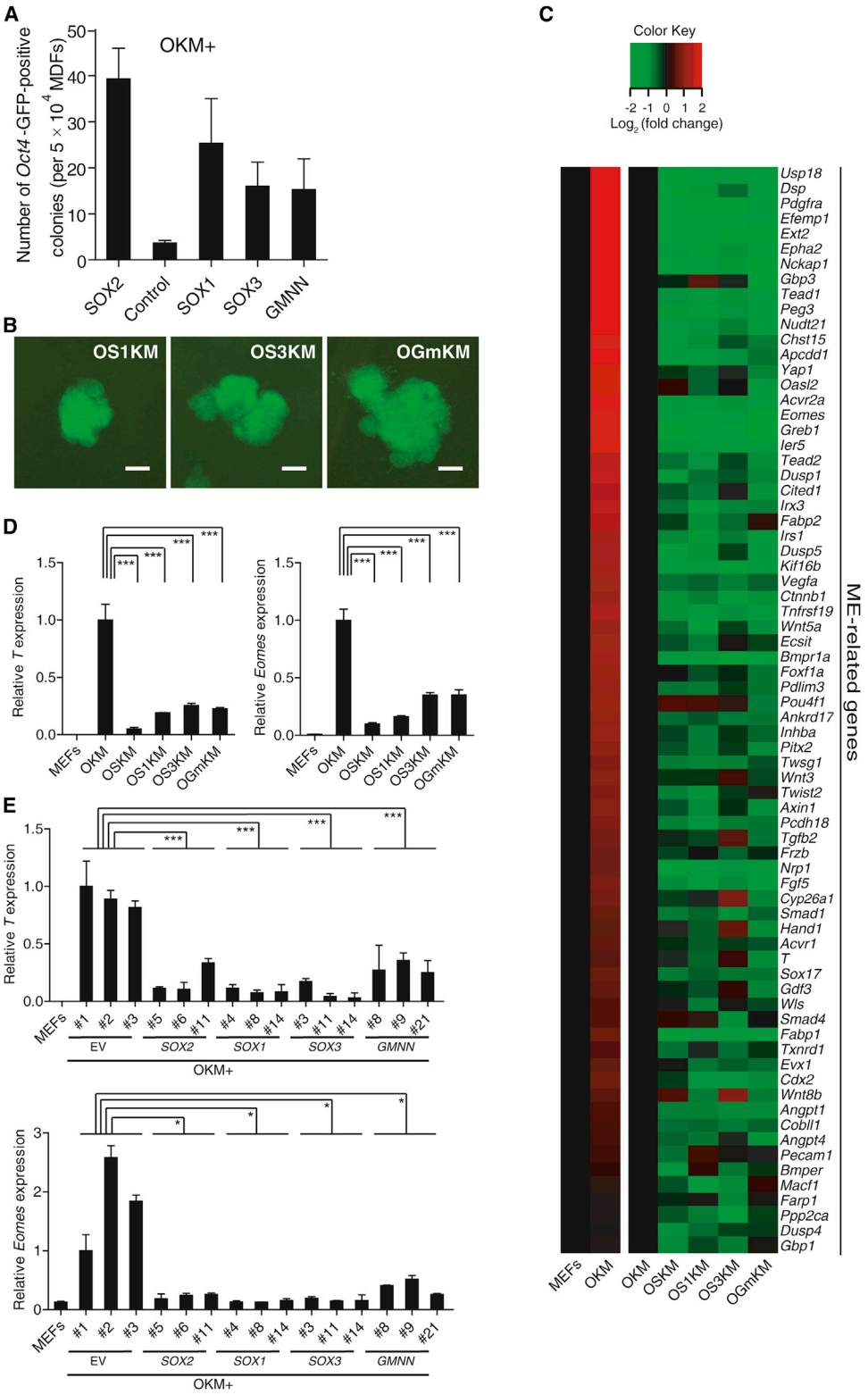

Figure 5. *SOX2* and Its Substitutes Attenuate the Expression of ME Genes that Are Elevated by OKM during Reprogramming

(A) Identification of lineage specifiers related to the ECT lineage that can facilitate reprogramming in the presence of OKM. The *Oct4*-GFP-positive colonies were counted at 9 dpi. OKM plus EV was used as a control. Error bars indicate the SD (n = 3).

(B) GFP images of iPS colonies generated with OKM+*SOX1* (OS1KM), OKM+*SOX3* (OS3KM), and OKM+*GMNN* (OGmKM). Scale bars, 100 μm.

(legend continued on next page)

model call for further investigation to validate or falsify the model.

One of the striking predictions of the model is that, when expressed together, an ME specifier and an ECT specifier can synergistically enhance reprogramming in the absence of both *OCT4* and *SOX2*. The mutually antagonistic nature of the differentiation module makes the system behave like an easily tilted "seesaw"; when the system tends to fall into either the ME or ECT state, in turn suppressing the pluripotency module, the cell is left with no chance to enter the pluripotency state. However, when both ME and ECT specifiers are exogenously expressed at appropriate levels, their external expression may be unable to compensate for the decrease in their endogenous expression due to the mutual inhibition. The differentiation module may end up in the balanced region, wherein neither ME specifiers nor ECT specifiers are present at levels that are sufficiently high to suppress the pluripotency module. Then, a self-activating pluripotency module may switch on by itself, eliciting the serial activation of a pluripotency network to realize successful reprogramming (Figures 6D, box v, S6G, and S6R–S6T).

To test the feasibility of this idea, we screened different combinations of lineage specifiers. We found that either (1) *GATA3*, *GATA6*, *PAX1*, and *SOX1* or *SOX3* or (2) *GATA6* plus *GMNN* can promote successful reprogramming without the two most critical pluripotency factors, *OCT4* and *SOX2* (Figures 6E, 6F, and S1E). Furthermore, these iPSCs were proven to be pluripotent (Figure S7). These lineage specifiers are not enriched in ESCs (Figure S1D), which indicates that the induction and maintenance of pluripotency may be two different scenarios.

DISCUSSION

Our data present the first evidence that the lineage specifiers *GATA3*, *GATA6*, *SOX7*, *PAX1*, *GATA4*, *CEBPa*, *HNF4a*, *GRB2*, and *GMNN*, which are generally considered as pluripotency rivals, can unexpectedly facilitate reprogramming and replace reprogramming factors of a corresponding lineage-specifying potential. We suggest a "seesaw model" in which lineage specifiers facilitate reprogramming when they are balanced with other mutually exclusive lineage specifiers. There are multiple ways to reach the pluripotency state, all involving balancing the forces that would otherwise drive the cell to a differentiated fate. Deviation from the balance directs cells to divergent differentiated states, reducing the possibility of restoring pluripotency. This hypothesis is complementary to previous studies demonstrating that lineage specifiers such as *Gata6*, a reported repressor of *Nanog*, hinder the reprogramming process (Chazaud et al., 2006; Mikkelsen et al., 2008). We suggest that pluripotency factors may direct lineage specification and that lineage specifiers may in turn influence the induction of pluripotency; this model provides the conceptually new perspective that one can reach the pluripotency "destination" by getting on cars that do not normally run at the destination.

Our "seesaw model" is in agreement with the recent perspective that pluripotency factors act as classical lineage-specifying factors to direct the differentiation of ESCs into a specific lineage while cross-inhibiting commitment to mutually exclusive lineages (Loh and Lim, 2011). The collaborative result is the temporary inhibition of all lineages to preserve an undifferentiated state. The self-activating pluripotency module could be activated when all of the lineage-specifying forces are counteracted, i.e., at the dynamic balanced point of the "seesaw," wherein no particular lineage-specifying activity is dominant to inhibit the pluripotency module. Once the pluripotency module is activated, the ME and ECT lineage fates are blocked by *SOX2* and *OCT4*, respectively, and the pluripotency state is maintained.

Most of these substitutes are usually depicted as typical ME markers (*GATA6*, *GATA4*, etc.) or ECT markers (*SOX1*, *SOX3*, etc.). To make our model succinct, these lineage specifiers are classified as either ME or ECT. However, this classification is not absolute, as indicated by our "seesaw model." The ME and ECT lineages are the two major counteracting lineages, but in the reprogramming symphony, an enormously intricate self-conflicted coalition of different lineage specifiers that are not limited to the ME and ECT lineages orchestrates the concerted induction of pluripotency.

The "seesaw model" focuses on one major aspect in reprogramming: understanding the implications of the reprogramming landscape that is shaped by the interactions among the different cell states. Needless to say, reprogramming is not merely a "seesaw." Several other important events, such as epigenetic changes, are also involved in this process. Furthermore, there are several important barriers to overcome for successful reprogramming. The various reprogramming factors execute their corresponding functions to facilitate the induction of pluripotency. Concomitantly, these factors may induce side effects, such as the stimulation of lineage specification. In addition to their reported functions in the activation of the pluripotency circuitry and in epigenetic and cell-cycle regulation, *KLF4* and *c-MYC* may also promote stimuli for particular lineages (Cao et al., 2012; Smith et al., 2010; Sridharan et al., 2009) to concert an equilibrium symphony. The function of these lineage specifiers may be involved in other processes and warrants further in-depth study.

We hope that our model can serve as a starting point to decipher the mysterious reprogramming code in a novel

(C) Heatmaps depicting the relative fold change of gene expression at 7 dpi based on the ME-related genes by microarray. Red and green indicate increased and decreased expression, respectively.

(D) RT-qPCR analysis of the expression of endogenous *T* (left) and *Eomes* (right) relative to the expression in OKM. Significance was assessed compared with the controls using a one-tailed Student's t test. ***$p < 0.001$. The samples were tested at 7 dpi. Error bars indicate the SD (n = 3).

(E) The expression of endogenous *T* (top) and *Eomes* (bottom) relative to the expression in OKM from a single colony; three colonies from each condition were tested. Significance was assessed compared with the controls using a one-tailed Student's t test. *$p < 0.05$, ***$p < 0.001$. Error bars indicate the SD (n = 3).

See also Figure S4 and Tables S2 and S4.

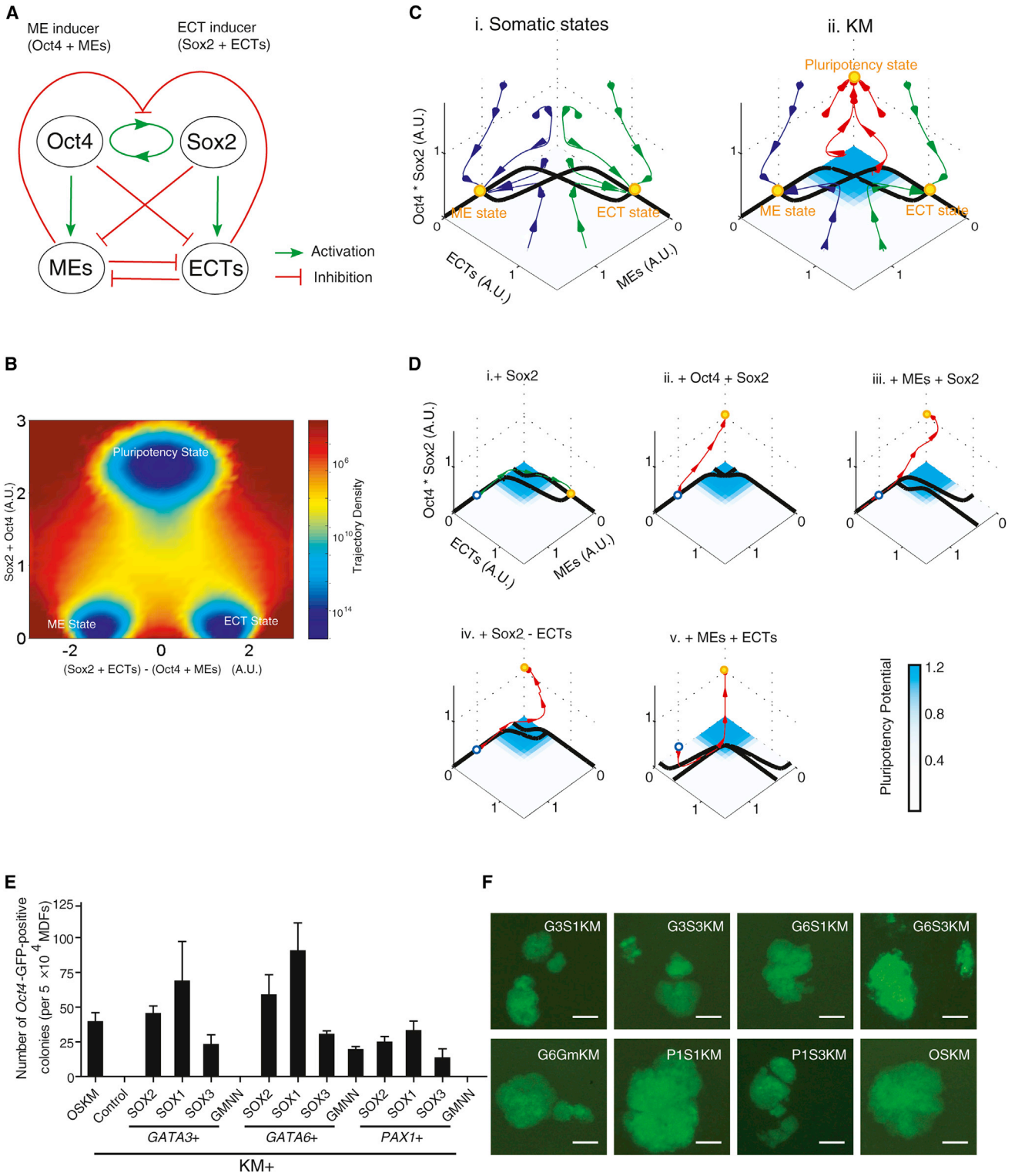

Figure 6. Balanced Equilibrium Facilitates the Induction of Pluripotency

(A) A model for the coupled pluripotency module (self-activation of *Oct4* and *Sox2*) and for the differentiation module (mutual antagonism between the ME and ECT lineages).

(B) The cell-state landscape obtained from the density of the trajectories. The blue color indicates deep "attractors" near which the cell states tend to stay. The x axis represents the difference between the two groups of lineage inducers, and the y axis indicates the "pluripotency" of the cell.

(legend continued on next page)

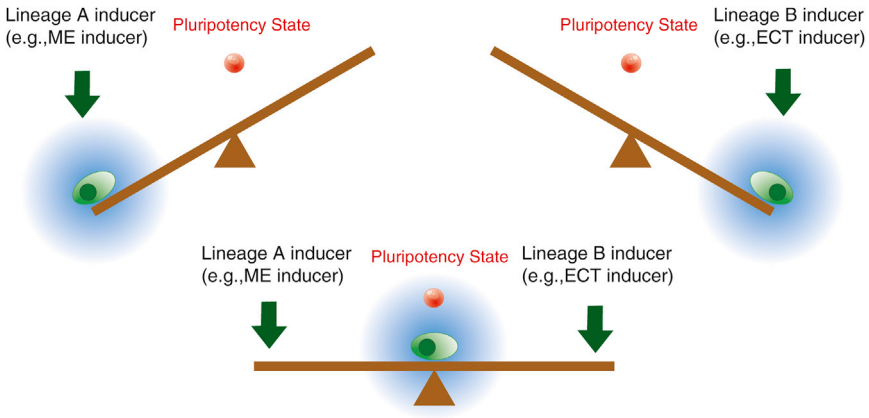

Figure 7. The "Seesaw Model"

A diagram of the "seesaw model." Blue clouds indicate the regions that the cell states are likely to sample with noise. The pluripotency state (red ball) is located near the balanced region. When the seesaw is balanced between the two differentiation potentials, the cell has a higher probability of entering the pluripotent state.

scenario. Our results suggest that a chemical screen for small molecules that can substitute for *OCT4* and *SOX2* in directing the corresponding lineage specification would be a novel and feasible strategy to generate iPSCs. Our findings also demonstrate the need for further investigation of the conventional perspectives regarding the functions of pluripotency factors and lineage specifiers and on the manner in which the pluripotency regulatory circuitry is established during reprogramming.

EXPERIMENTAL PROCEDURES

Screen

The 10,080 cDNAs that were screened for their ability to replace *OCT4* were obtained from Origene Co., Ltd. *Oct4*-GFP MEFs were infected with SKM (*SOX2*, *KLF4*, and *c-MYC*) lentiviral supernatant (MOI: 4) supplemented with 10 ng/μl polybrene (Sigma) for 12 hr. Details are provided in the Extended Experimental Procedures.

Cell Culture

Primary MEFs, mouse GECs, keratinocytes, and MDFs were derived from ICR × *Oct4*-GFP transgenic mice. Mouse GECs were isolated and cultured as previously described (Aoi et al., 2008). Details are provided in the Extended Experimental Procedures.

iPSCs Generation

The dox-inducible lentiviral system used has been previously described (Maherali et al., 2008). Further details are provided in the Extended Experimental Procedures.

Time Course of *GATA3* Induction

A dox-inducible lentiviral system was used, so the expression of tet-*GATA3*, but not pll3.7-ΔU6ΔGFP-*SOX2*, pll3.7-ΔU6ΔGFP-*KLF4*, or pll3.7-ΔU6ΔGFP-*c-MYC* (Zhao et al., 2008), could be induced by dox. Dox was added to the culture medium for different periods of time, and the number of *Oct4*-GFP-positive colonies was counted at 10 dpi.

Characterization of iPSCs

The teratoma formation and chimera experiments were performed as previously described (Li et al., 2011). The primers used for RT-PCR, genomic PCR, and RT-qPCR are listed in Table S7. Bisulfite treatment of DNA was performed using the CpGenome Fast DNA Modification Kit (Millipore). The primers used for promoter fragment amplification have been previously described (Takahashi and Yamanaka, 2006). The details for immunofluorescence and the detection of AP activity are provided in the Extended Experimental Procedures.

Single-Colony Analysis

Five days after infection with different reprogramming cocktails, Alkaline Phosphatase Live Stain (Invitrogen) was used for the detection of AP activity. AP-positive colonies were then picked, and each colony was divided into two parts. One part was kept culturing in induction medium for 2–4 days. The other part was frozen at −80°C. If *Oct4*-GFP turned on after an additional 2–4 days induction and became dox independent in 4 days without dox, total RNA was isolated from the frozen part using the RNeasy micro kit (QIAGEN) and then used for RT-qPCR analysis.

Knockdowns

Dlx3 knockdown was achieved using shRNA lentiviral vectors (Sigma) containing a puromycin resistance gene. Further details are provided in the Extended Experimental Procedures.

Western Blotting

Cells were washed with PBS, treated with 1 × SDS sample buffer, and then boiled. Additional details are provided in the Extended Experimental Procedures.

DNA Microarray

Total mRNA from iPSCs, MEFs, MEFs at 7 dpi, and R1 were labeled with Cy5 hybridized to a mouse oligo microarray (Phalanx Mouse Whole Genome OneArray; Phalanx Biotech). The data were analyzed according to the manufacturer's protocol.

RNA-Seq

RNA-sequencing libraries were constructed using the Illumina mRNA-seq Prep Kit. The fragmented and randomly primed 200 bp paired-end libraries

(C and D) The phase space without (box i)/with KM (box ii) under no input, respectively (C). Different reprogramming strategies with KM and the trajectory starting from the ME state are shown (D). The blue circuit indicates the ME state where the trajectories start. Yellow dots indicate stable cell states. The changing directions of cell states are marked by arrows. The trajectories that end up in the ME state, the ECT state, and the pluripotent state are colored by blue, green, and red, respectively. Cyan indicates the region where the reprogramming is possible. Dark lines are the nullclines of the differentiation module when the pluripotency module is OFF. When the stable crossing point falls into the cyan reprogramming region, pluripotency can be restored.

(E) The generation of mouse iPSCs in the absence of both *OCT4* and *SOX2*. KM plus EV was used as a control. The *Oct4*-GFP-positive colonies were counted at 9 dpi. Error bars indicate the SD (n = 3).

(F) GFP images of iPS colonies generated with KM+*GATA3*+*SOX1* (G3S1KM), KM+*GATA3*+*SOX3* (G3S3KM), KM+*GATA6*+*SOX1* (G6S1KM), KM+*GATA6*+*SOX3* (G6S3KM), KM+*GATA6*+*GMNN* (G6GmKM), KM+*PAX1*+*SOX1* (P1S1KM), KM+*PAX1*+*SOX3* (P1S3KM), and OSKM. Scale bars, 100 μm.

See also Figures S6 and S7 and Tables S5 and S6.

were sequenced using Illumina HiSeq 2000. Details are included in the Extended Experimental Procedures.

Statistical Analysis

Cell proliferation curves were analyzed using a paired two-tailed Student's t test. The unpaired one-tailed t test was used for statistical analysis of other experiments. The standard deviation (SD) was used to quantify variability.

Model Construction

A coarse-grained model was built based on our results and the results of previous studies. The interactions involved in this model are illustrated in Figure 6A. Additional details are provided in the Extended Experimental Procedures.

ACCESSION NUMBERS

Microarray and RNA-seq data are available in the Gene Expression Omnibus (GEO) database (http://www.ncbi.nlm.nih.gov/geo/) under the accession number GSE43995.

SUPPLEMENTAL INFORMATION

Supplemental Information includes the Extended Experimental Procedures, seven figures, and seven tables and can be found with this article online at http://dx.doi.org/10.1016/j.cell.2013.05.001.

ACKNOWLEDGMENTS

We thank Chengyan Wang and Xiaolei Yin for helpful discussions. We also thank Haisong Liu, Jiancheng Wang, Zhiyuan Hou, Ren Li, Fangfang Zhu, Dongyi Xu, and Xing Zhang for technical assistance. J.S., C.W., and Y.W. conducted most of the experiments in this study. Z.L. performed the computer analysis and mathematical model analysis. H.D., Y.Z., and C.T. conceived of and supervised the study. This work was supported by grants from the National Basic Research Program of China (973 program grant numbers 2012CB966401, 2009CB941101, 2010CB945204, and 2009CB918500), the Key New Drug Creation and Manufacturing Program (grant numbers 2011ZX09102-010-03), the National Natural Science Foundation of China (grant numbers 90919031 and 11021463), the 111 project, and NSF (CMMI-0941355).

Received: October 26, 2012
Revised: February 13, 2013
Accepted: April 15, 2013
Published: May 23, 2013

REFERENCES

Aoi, T., Yae, K., Nakagawa, M., Ichisaka, T., Okita, K., Takahashi, K., Chiba, T., and Yamanaka, S. (2008). Generation of pluripotent stem cells from adult mouse liver and stomach cells. Science *321*, 699–702.

Boyer, L.A., Lee, T.I., Cole, M.F., Johnstone, S.E., Levine, S.S., Zucker, J.P., Guenther, M.G., Kumar, R.M., Murray, H.L., Jenner, R.G., et al. (2005). Core transcriptional regulatory circuitry in human embryonic stem cells. Cell *122*, 947–956.

Buganim, Y., Faddah, D.A., Cheng, A.W., Itskovich, E., Markoulaki, S., Ganz, K., Klemm, S.L., van Oudenaarden, A., and Jaenisch, R. (2012). Single-cell expression analyses during cellular reprogramming reveal an early stochastic and a late hierarchic phase. Cell *150*, 1209–1222.

Cao, Q., Zhang, X., Lu, L., Yang, L., Gao, J., Gao, Y., Ma, H., and Cao, Y. (2012). Klf4 is required for germ-layer differentiation and body axis patterning during Xenopus embryogenesis. Development *139*, 3950–3961.

Chazaud, C., Yamanaka, Y., Pawson, T., and Rossant, J. (2006). Early lineage segregation between epiblast and primitive endoderm in mouse blastocysts through the Grb2-MAPK pathway. Dev. Cell *10*, 615–624.

Chia, N.-Y., Chan, Y.-S., Feng, B., Lu, X., Orlov, Y.L., Moreau, D., Kumar, P., Yang, L., Jiang, J., Lau, M.-S., et al. (2010). A genome-wide RNAi screen reveals determinants of human embryonic stem cell identity. Nature *468*, 316–320.

Doege, C.A., Inoue, K., Yamashita, T., Rhee, D.B., Travis, S., Fujita, R., Guarnieri, P., Bhagat, G., Vanti, W.B., Shih, A., et al. (2012). Early-stage epigenetic modification during somatic cell reprogramming by Parp1 and Tet2. Nature *488*, 652–655.

Graf, T., and Enver, T. (2009). Forcing cells to change lineages. Nature *462*, 587–594.

Gu, P., Goodwin, B., Chung, A.C.K., Xu, X., Wheeler, D.A., Price, R.R., Galardi, C., Peng, L., Latour, A.M., Koller, B.H., et al. (2005). Orphan nuclear receptor LRH-1 is required to maintain Oct4 expression at the epiblast stage of embryonic development. Mol. Cell. Biol. *25*, 3492–3505.

Guo, G., and Smith, A. (2010). A genome-wide screen in EpiSCs identifies Nr5a nuclear receptors as potent inducers of ground state pluripotency. Development *137*, 3185–3192.

Han, D.W., Tapia, N., Hermann, A., Hemmer, K., Höing, S., Araúzo-Bravo, M.J., Zaehres, H., Wu, G., Frank, S., Moritz, S., et al. (2012). Direct reprogramming of fibroblasts into neural stem cells by defined factors. Cell Stem Cell *10*, 465–472.

Hanna, J., Saha, K., Pando, B., van Zon, J., Lengner, C.J., Creyghton, M.P., van Oudenaarden, A., and Jaenisch, R. (2009). Direct cell reprogramming is a stochastic process amenable to acceleration. Nature *462*, 595–601.

Heng, J.-C.D., Feng, B., Han, J., Jiang, J., Kraus, P., Ng, J.-H., Orlov, Y.L., Huss, M., Yang, L., Lufkin, T., et al. (2010). The nuclear receptor Nr5a2 can replace Oct4 in the reprogramming of murine somatic cells to pluripotent cells. Cell Stem Cell *6*, 167–174.

Huang, S. (2009). Reprogramming cell fates: reconciling rarity with robustness. Bioessays *31*, 546–560.

Jaenisch, R., and Young, R. (2008). Stem cells, the molecular circuitry of pluripotency and nuclear reprogramming. Cell *132*, 567–582.

Jopling, C., Boue, S., and Izpisua Belmonte, J.C. (2011). Dedifferentiation, transdifferentiation and reprogramming: three routes to regeneration. Nat. Rev. Mol. Cell Biol. *12*, 79–89.

Kim, J., Chu, J., Shen, X., Wang, J., and Orkin, S.H. (2008). An extended transcriptional network for pluripotency of embryonic stem cells. Cell *132*, 1049–1061.

Li, R., Liang, J., Ni, S., Zhou, T., Qing, X., Li, H., He, W., Chen, J., Li, F., Zhuang, Q., et al. (2010). A mesenchymal-to-epithelial transition initiates and is required for the nuclear reprogramming of mouse fibroblasts. Cell Stem Cell *7*, 51–63.

Li, Y., Zhang, Q., Yin, X., Yang, W., Du, Y., Hou, P., Ge, J., Liu, C., Zhang, W., Zhang, X., et al. (2011). Generation of iPSCs from mouse fibroblasts with a single gene, Oct4, and small molecules. Cell Res. *21*, 196–204.

Loh, K.M., and Lim, B. (2011). A precarious balance: pluripotency factors as lineage specifiers. Cell Stem Cell *8*, 363–369.

Maekawa, M., Yamaguchi, K., Nakamura, T., Shibukawa, R., Kodanaka, I., Ichisaka, T., Kawamura, Y., Mochizuki, H., Goshima, N., and Yamanaka, S. (2011). Direct reprogramming of somatic cells is promoted by maternal transcription factor Glis1. Nature *474*, 225–229.

Maherali, N., Ahfeldt, T., Rigamonti, A., Utikal, J., Cowan, C., and Hochedlinger, K. (2008). A high-efficiency system for the generation and study of human induced pluripotent stem cells. Cell Stem Cell *3*, 340–345.

Mikkelsen, T.S., Hanna, J., Zhang, X.L., Ku, M.C., Wernig, M., Schorderet, P., Bernstein, B.E., Jaenisch, R., Lander, E.S., and Meissner, A. (2008). Dissecting direct reprogramming through integrative genomic analysis. Nature *454*, 49–55.

Nakagawa, M., Koyanagi, M., Tanabe, K., Takahashi, K., Ichisaka, T., Aoi, T., Okita, K., Mochiduki, Y., Takizawa, N., and Yamanaka, S. (2008). Generation of induced pluripotent stem cells without Myc from mouse and human fibroblasts. Nat. Biotechnol. *26*, 101–106. Published online November 30, 2007. http://dx.doi.org/10.1038/nbt1374.

Niakan, K.K., Ji, H., Maehr, R., Vokes, S.A., Rodolfa, K.T., Sherwood, R.I., Yamaki, M., Dimos, J.T., Chen, A.E., Melton, D.A., et al. (2010). Sox17 promotes differentiation in mouse embryonic stem cells by directly regulating extraembryonic gene expression and indirectly antagonizing self-renewal. Genes Dev. *24*, 312–326.

Nishiyama, A., Xin, L., Sharov, A.A., Thomas, M., Mowrer, G., Meyers, E., Piao, Y., Mehta, S., Yee, S., Nakatake, Y., et al. (2009). Uncovering early response of gene regulatory networks in ESCs by systematic induction of transcription factors. Cell Stem Cell *5*, 420–433.

Niwa, H., Miyazaki, J., and Smith, A.G. (2000). Quantitative expression of Oct-3/4 defines differentiation, dedifferentiation or self-renewal of ES cells. Nat. Genet. *24*, 372–376.

Pardo, M., Lang, B., Yu, L., Prosser, H., Bradley, A., Babu, M.M., and Choudhary, J. (2010). An expanded Oct4 interaction network: implications for stem cell biology, development, and disease. Cell Stem Cell *6*, 382–395.

Polo, J.M., Anderssen, E., Walsh, R.M., Schwarz, B.A., Nefzger, C.M., Lim, S.M., Borkent, M., Apostolou, E., Alaei, S., Cloutier, J., et al. (2012). A molecular roadmap of reprogramming somatic cells into iPS cells. Cell *151*, 1617–1632.

Ring, K.L., Tong, L.M., Balestra, M.E., Javier, R., Andrews-Zwilling, Y., Li, G., Walker, D., Zhang, W.R., Kreitzer, A.C., and Huang, Y. (2012). Direct reprogramming of mouse and human fibroblasts into multipotent neural stem cells with a single factor. Cell Stem Cell *11*, 100–109.

Rosa, A., and Brivanlou, A.H. (2011). A regulatory circuitry comprised of miR-302 and the transcription factors OCT4 and NR2F2 regulates human embryonic stem cell differentiation. EMBO J. *30*, 237–248. Published online December 10, 2010. http://dx.doi.org/10.1038/emboj.2010.319.

Samavarchi-Tehrani, P., Golipour, A., David, L., Sung, H.K., Beyer, T.A., Datti, A., Woltjen, K., Nagy, A., and Wrana, J.L. (2010). Functional genomics reveals a BMP-driven mesenchymal-to-epithelial transition in the initiation of somatic cell reprogramming. Cell Stem Cell *7*, 64–77.

Seo, S., Herr, A., Lim, J.W., Richardson, G.A., Richardson, H., and Kroll, K.L. (2005). Geminin regulates neuronal differentiation by antagonizing Brg1 activity. Genes Dev. *19*, 1723–1734.

Silva, J., Nichols, J., Theunissen, T.W., Guo, G., van Oosten, A.L., Barrandon, O., Wray, J., Yamanaka, S., Chambers, I., and Smith, A. (2009). Nanog is the gateway to the pluripotent ground state. Cell *138*, 722–737.

Smith, K.N., Singh, A.M., and Dalton, S. (2010). Myc represses primitive endoderm differentiation in pluripotent stem cells. Cell Stem Cell *7*, 343–354.

Sridharan, R., Tchieu, J., Mason, M.J., Yachechko, R., Kuoy, E., Horvath, S., Zhou, Q., and Plath, K. (2009). Role of the murine reprogramming factors in the induction of pluripotency. Cell *136*, 364–377.

Szabo, E., Rampalli, S., Risueño, R.M., Schnerch, A., Mitchell, R., Fiebig-Comyn, A., Levadoux-Martin, M., and Bhatia, M. (2010). Direct conversion of human fibroblasts to multilineage blood progenitors. Nature *468*, 521–526.

Takahashi, K., and Yamanaka, S. (2006). Induction of pluripotent stem cells from mouse embryonic and adult fibroblast cultures by defined factors. Cell *126*, 663–676.

Teo, A.K.K., Arnold, S.J., Trotter, M.W.B., Brown, S., Ang, L.T., Chng, Z., Robertson, E.J., Dunn, N.R., and Vallier, L. (2011). Pluripotency factors regulate definitive endoderm specification through eomesodermin. Genes Dev. *25*, 238–250.

Thier, M., Wörsdörfer, P., Lakes, Y.B., Gorris, R., Herms, S., Opitz, T., Seiferling, D., Quandel, T., Hoffmann, P., Nöthen, M.M., et al. (2012). Direct conversion of fibroblasts into stably expandable neural stem cells. Cell Stem Cell *10*, 473–479.

Thomson, M., Liu, S.J., Zou, L.N., Smith, Z., Meissner, A., and Ramanathan, S. (2011). Pluripotency factors in embryonic stem cells regulate differentiation into germ layers. Cell *145*, 875–889.

Ting, C.N., Olson, M.C., Barton, K.P., and Leiden, J.M. (1996). Transcription factor GATA-3 is required for development of the T-cell lineage. Nature *384*, 474–478.

Tontsch, S., Zach, O., and Bauer, H.-C. (2001). Identification and localization of M-CoREST (1A13), a mouse homologue of the human transcriptional co-repressor CoREST, in the developing mouse CNS. Mech. Dev. *108*, 165–169.

Vierbuchen, T., and Wernig, M. (2011). Direct lineage conversions: unnatural but useful? Nat. Biotechnol. *29*, 892–907.

Wang, Z., Oron, E., Nelson, B., Razis, S., and Ivanova, N. (2012). Distinct lineage specification roles for NANOG, OCT4, and SOX2 in human embryonic stem cells. Cell Stem Cell *10*, 440–454.

Wernig, M., Lengner, C.J., Hanna, J., Lodato, M.A., Steine, E., Foreman, R., Staerk, J., Markoulaki, S., and Jaenisch, R. (2008). A drug-inducible transgenic system for direct reprogramming of multiple somatic cell types. Nat. Biotechnol. *26*, 916–924.

Yang, P., Wang, Y., Chen, J., Li, H., Kang, L., Zhang, Y., Chen, S., Zhu, B., and Gao, S. (2011). RCOR2 is a subunit of the LSD1 complex that regulates ESC property and substitutes for SOX2 in reprogramming somatic cells to pluripotency. Stem Cells *29*, 791–801.

Young, R.A. (2011). Control of the embryonic stem cell state. Cell *144*, 940–954.

Yu, J., Vodyanik, M.A., Smuga-Otto, K., Antosiewicz-Bourget, J., Frane, J.L., Tian, S., Nie, J., Jonsdottir, G.A., Ruotti, V., Stewart, R., et al. (2007). Induced pluripotent stem cell lines derived from human somatic cells. Science *318*, 1917–1920.

Zeng, W., Kong, Q., Li, C., and Mao, B. (2010). Xenopus RCOR2 (REST corepressor 2) interacts with ZMYND8, which is involved in neural differentiation. Biochem. Biophys. Res. Commun. *394*, 1024–1029.

Zhao, Y., Yin, X., Qin, H., Zhu, F., Liu, H., Yang, W., Zhang, Q., Xiang, C., Hou, P., Song, Z., et al. (2008). Two supporting factors greatly improve the efficiency of human iPSC generation. Cell Stem Cell *3*, 475–479.

Zhu, S., Li, W., Zhou, H., Wei, W., Ambasudhan, R., Lin, T., Kim, J., Zhang, K., and Ding, S. (2010). Reprogramming of human primary somatic cells by OCT4 and chemical compounds. Cell Stem Cell *7*, 651–655.